Brandon Balamut
Investigating Coacervate Drug Delivery Systems with NMR

Abstract

Pulsed field gradient nuclear magnetic resonance was used to study the diffusion of poly(diallyldimethylammonium chloride), ^{19}F, ^{23}Na, and ^{35}Cl nuclei in the coacervates formed from this polycation and the protein bovine serum albumin. Heterogeneity of the coacervate was confirmed with diffusion measurements and supports the theory of microscopic regions correlating to the dense domains, breaking up of the dense domains, and less dense domains. Ion diffusivity findings are discussed in relationship to the heterogeneous domains and provide information for future use of soft drug delivery systems.

Background

As the search for a better drug delivery method in the body continues, clinical applications for polymeric drug carriers have been developed for the benefits of controlled drug release and the reduction of drug resistance [1]. Various forms of so-called "soft matter" such as polymers, hydrogels, liposomes, and polyelectrolyte complexes have been studied as drug delivery vehicles because they can be prepared at the nanoscale level, have high-drug loading capacities, control drug release rates, and have surfaces that are easily modifiable [2].

Examinations of biphasic systems, such as lyophobic colloids, have shown much promise in targeted drug delivery. Ionic polymers exist in aqueous solution surrounded by a double layer of ions of opposite charge. When two oppositely charged ionic polymers are mixed, a biphasic polyelectrolyte complex driven by an increase in entropy is formed and the electrical double layer surrounding the macro-ions is partially destroyed, releasing counterions into solution. Upon centrifugation, a dense phase of a high concentration of polymers is formed beneath a less dense supernatant layer of low concentration of polymers. Many of the challenges working with polyelectrolyte complexes include understanding how various factors influence the relevant properties of these systems: pH, charge density, chemical groups, and ionic strength of solution.

Coacervation is not limited to oppositely charged polyelectrolytes, but can form when one of the components is a colloidal particle such as a protein. Polyelectrolyte-protein complexation is driven electrostatically and the degree of complexation increases as the linear charge density of the polymer and surface density of the protein increases. Previous studies of polyelectrolyte-protein coacervation focused on microencapsulation of pharmaceutical agents [3] and enzymes [4], but information regarding the dynamic association and microstructure of polyelectrolyte-protein coacervates is still lacking.

Recent studies of coacervates prepared with the protein, bovine serum albumin (BSA), and cationic polymer poly(diallyldimethylammonium chloride) (PDADMAC), have provided information suggesting a mesophase separation within the coacervate. Fluorescence recovery after photobleaching (FRAP) and dynamic light scattering (DLS) reveal multiple modes of protein diffusion with diffusion coefficients slightly smaller than dilute protein even though the large difference in viscosity [5]. Observations by cryo-TEM indicate areas of protein-rich domains between the length of tens and hundreds of nanometers [6].

While scattering experiments can only measure diffusion of the protein due to the large dominant signal, pulsed-field gradient nuclear magnetic resonance (PFG NMR) experiments can measure the diffusion of the polymer and various ions present. Previous ^{1}H PFG NMR studies have confirmed diffusion heterogeneity of PDADMAC inside the coacervate but no data has been presented about ion diffusivity or whether there is a corresponding heterogeneity of ion diffusion [6].

In the present study, a narrow molecular weight of PDADMAC was synthesized from diallyldimethylammonium chloride (DADMAC) using 2 2'-azobis(2-methylpropionamidine) dihydrochloride as the initiator, and confirmed using size-exclusion chromatography. PDADMAC chloride ions were exchanged with trifluoroacetate ions and two coacervate samples were created: one PDADMAC/BSA coacervate and one PDADMAC/TFA/BSA coacervate. PFG NMR diffusion was carried out for the following nuclei to confirm coacervate heterogeneity and to investigate diffusion for the polyelectrolyte and ions in the coacervate: ^{1}H, ^{19}F, ^{23}Na, and ^{35}Cl.

Experimental Section

Synthesis and Purification of PDADMAC. PDADMAC samples of M_w 191446 g/mol (M_n 147676 g/mol) and M_w 187673 g/mol (M_n 136761 g/mol) were synthesized by free radical cyclopolymerization (Fig. 1). All polymerizations were carried out in aqueous solution using 2 2'-azobis(2-methylpropionamidine) as the initiator and diallyldimethylammonium chloride as the monomer [7]. Monomer concentration was 0.6M, initiator concentration was 0.06M, and the reaction temperature was 45°C. The reaction was carried out in a sealed three-neck round bottom flask for 8 hours. Preceding cyclopolymerization, monomer and initiator were purged under nitrogen gas for 2 hours. The monomer temperature was raised to reaction temperature before the initiator was mixed. The polymerization was stopped at low conversion by diluting and cooling to avoid chain branching. PDADMAC was purified using 80mL Centricon spin columns, MW cutoff 30,000 g/mol. Samples were lyophilized using a Labconco Lyophillizer.

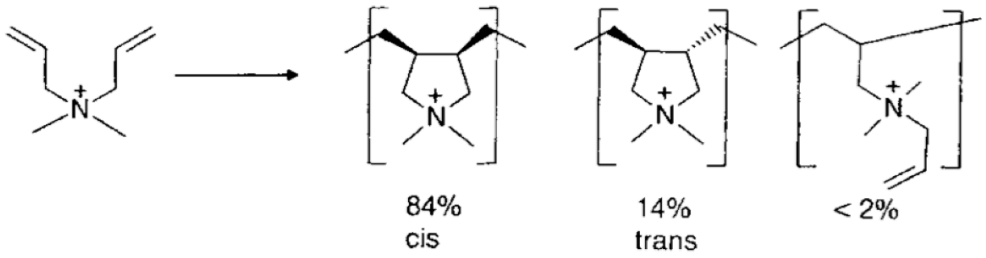

Figure 1: Chemical Structure of PDADMAC via free radical cyclopolymerization [7].

Analytical Size-Exclusion Chromatography. HPLC measurements were carried out using the Agilent 1100 HPLC System with a Showdex OHpak SB-804 HQ column. The mobile phase was 0.5M acetate buffer, 0.3M sodium nitrate, at pH 3. PDADMAC

samples were analyzed using an Agilent 1100 Refractive Index Detector. Samples were filtered using Spartan 13 0.45 µm filter units, manufactured by Whatman. Injection volumes were 20µL.

Polyethylene glycol standards (*Agilent Technologies)* of known molecular weight were used to make a calibration curve (Fig. 2). PDADMAC samples were analyzed and the molecular weight was determined from the 3rd degree polynomial fit.

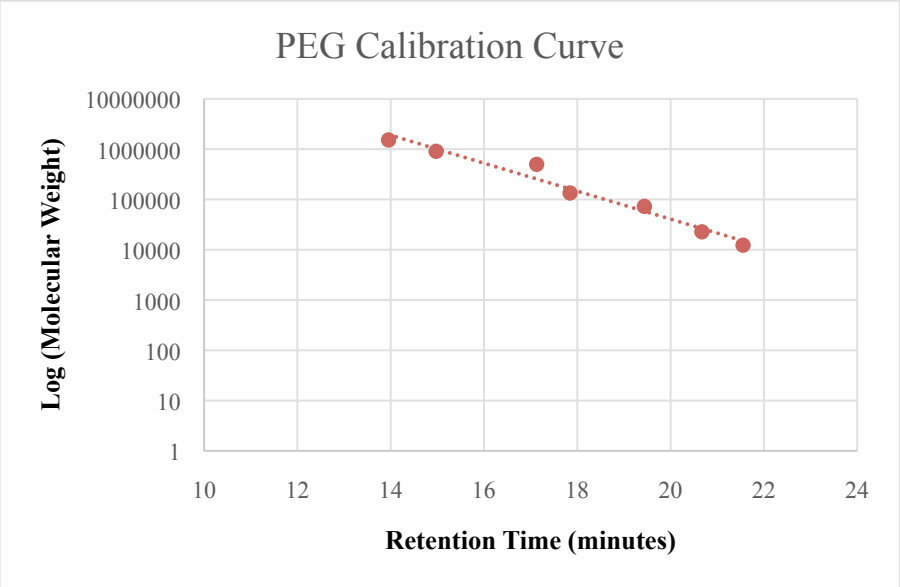

Figure 2: Polyethylene glycol calibration curve with 3rd degree polynomial fit. Equation: $y= -0.014982x^2+0.25357x+5.5569$

Ion Exchange. The PDADMAC counterion, chloride, was exchanged with trifluoroacetate using 80mL Centricon spin column preceding centrifugation at 4000xG. A solution of 0.1M sodium trifluoroacetate was exchanged after each centrifugation and repeated.

Coacervate Preparation. BSA (6mg/mL) and PDADMAC (1.2mg/mL) were prepared separately in 0.1M NaCl. The pH of each solution was adjusted to 4 with 6M HCl prior to mixing to limit interaction of BSA with PDADMAC. Equal volumes were mixed and the pH was gradually raised to 8.5 using 6M NaOH. The mixture was centrifuged at 4000xG and a majority of supernatant was decanted. The coacervate solution was centrifuged at 4000xG one further time. A second sample of BSA and ion-exchanged PDADMAC was also prepared separately in 0.1M sodium trifluoroacetate and used to make coacervate.

In order to minimize the water signal during NMR experiments, D_2O was exchanged with water inside of the coacervate multiple times. A sample of D_2O, pH 8.5, in 0.1M NaCl was placed above coacervate and vortexed for 20 minutes preceding centrifugation at 4000xG for 20 minutes. Coacervate was placed into a NMR tube with small amount of supernatant left in tube.

Analytical NMR. ^{1}H, ^{19}F, and ^{23}Na PFG NMR diffusion data was measured on a wide-bore Bruker Avance III 400 MHz (9.4 T) NMR equipped with a Diff60 diffusion probe with exchangeable coil inserts (Bruker Biospin, Billerica, MA). ^{1}H and ^{19}F were measured with a 5 mm ^{1}H/^{19}F coil. ^{23}Na was measured with a 5 mm ^{23}Na coil. ^{35}Cl was measured on a Bruker Avance III 600 MHz (14.1 T) spectrometer using a Doty 20-40 C multinuclear diffusion probe (Doty Scientific, Columbia, SC).

The pulsed-gradient stimulated echo (PGSTE) sequence was used to measure diffusion, with an effective gradient pulse length of δ = 2 ms (3 ms for ^{35}Cl), gradient pulse spacing of Δ = 50 ms (30 ms for ^{23}Na, 8 ms for ^{35}Cl), and maximum gradient strengths ranging from g = 40 G/cm to g = 1800 G/cm. 12−24 gradient steps were applied, and the number of scans varied from 4 to 64 for adequate signal-to-noise ratios. Diffusion was measured along the spectrometer magnetic field ($B_0 = z$) direction. A series of NMR spectra were recorded as a function of gradient strength and fit to the Stejskal-Tanner equation,

$$I = I_0 e^{-D\gamma^2 g^2 \delta^2 (\Delta - \delta/3)}$$

where D is the measured diffusion coefficient and γ is the gyromagnetic ratio of the nucleus.

Results and Discussion

Comparisons of ^{1}H NMR spectra recorded by free-induction decay (FID) are shown in Figure 3. The broader peak widths in the NMR spectra can be attributed to the rotationally restricted mobility of the portion of the molecule. This can be seen when comparing the NMR spectra of isolated solutions of BSA (Figure 3, bottom) and PDADMAC (Figure 3, second from bottom). Between 0 and 2 ppm, the peaks in the BSA spectrum are very broad due to the structural rigidity of the 66,483 g/mol globular protein. Although the molecular mass of PDADMAC is close to three times greater (~190,000 g/mol) than the BSA protein, the narrow peaks in the spectrum are due to the flexibility of the linear polymer chain. The ^{1}H NMR spectrum from the coacervate (Figure 3, top) contains similar features to the PDADMAC spectrum, however the spectrum is considerably broadened due to the reduced mobility of PDADMAC inside the coacervate. The water peak assigned to 4.8 ppm is wider in the coacervate than in the polymer or protein solutions due to the slower rotational mobility of the water inside the denser coacervate phase.

Also contained in Figure 3 (second from top) is a one-dimensional spectrum of the coacervate taken with the pulsed-gradient stimulated echo sequence. Diffusion coefficients of nuclei with short T_2 relaxation times do not appear in the spectra, which can be visualized by comparing the coacervate spectrum (Figure 3, top) and the diffusion slice (Figure 3, second from top). The underlying broad component is no longer present and thus has great implications for the interpretation of our diffusion experiments.

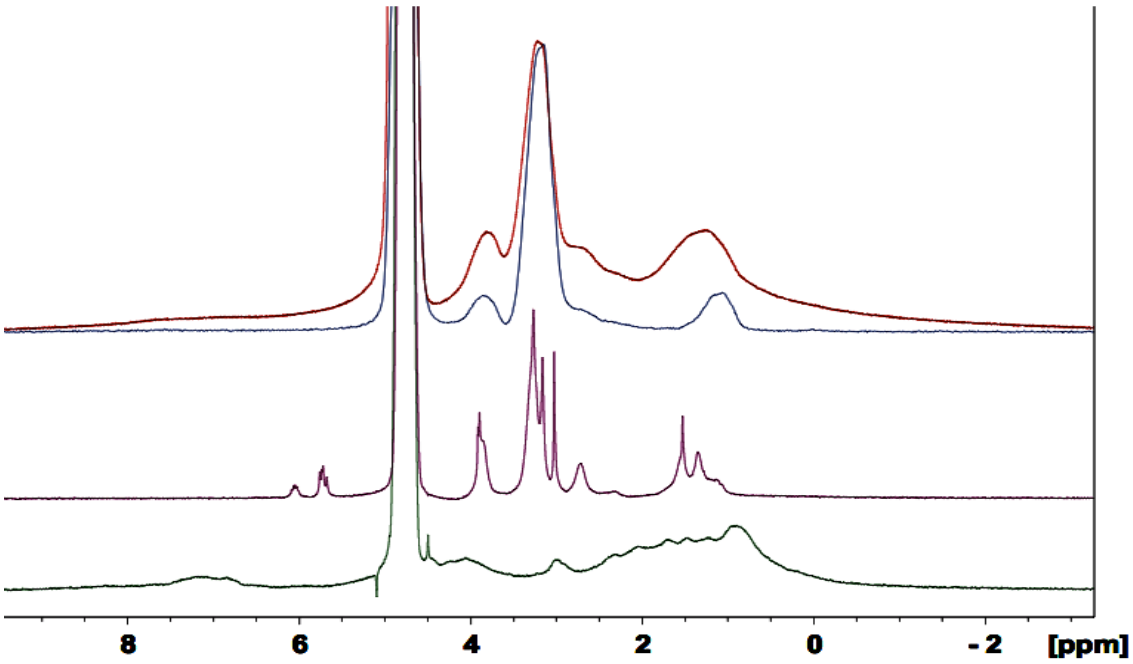

Figure 3: ^{1}H NMR frequency-domain of PDADMAC-BSA coacervate and components that make up coacervate. Red (top): PDADMAC-BSA Coacervate, Blue (second from top): PDADMAC-BSA Coacervate Diffusion Slice, Pink (second from bottom): PDADMAC, Green (bottom): BSA Protein

Compared with PDADMAC solution, diffusion coefficients were not similar to coacervate, confirming that diffusion measurements were not from the supernatant of the NMR tube, but from the coacervate (Fig. 4). The attenuation curves for PDADMAC-BSA coacervate hinted that diffusion measurements were measured for more than one component inside the coacervate for the polyelectrolyte (Fig. 5). Figure 6 demonstrates that another component is present based off the poor attenuation fit, which means that in the coacervate phase there are at least two rates of PDADMAC diffusion. From previous scattering and cryo-TEM studes [5] it is known that both dilute and dense phases exist within the coacervate phase and the two-component fit confirms the heterogeneity inside the coacervate. 93.5% of the diffusion measurement inside the PDADMAC-BSA coacervate can be attributed to the less dense regions inside the coacervate. The other component representing 6.5% of the diffusion measurement can be attributed to the breaking up of the dense regions inside the coacervate. Based on theories of diffusion, the movement from areas of high concentration to low concentration allows faster polymer movement than in the less dense regions. From PGSTE, a short transverse relaxation time hints at a third component inside the coacervate phase that is not being measured. This diffusion coefficient is thought to be polymer inside the dense regions of the coacervate and longer gradient pulse lengths would be needed to get diffusion information. Diffusion measurements for PDADMAC-TFA coacervate only showed one component in the less dense region of the coacervate. It is suggested that there are two components, possibly three, but data was inconclusive due to time constraints and further experiments should be able to verify.

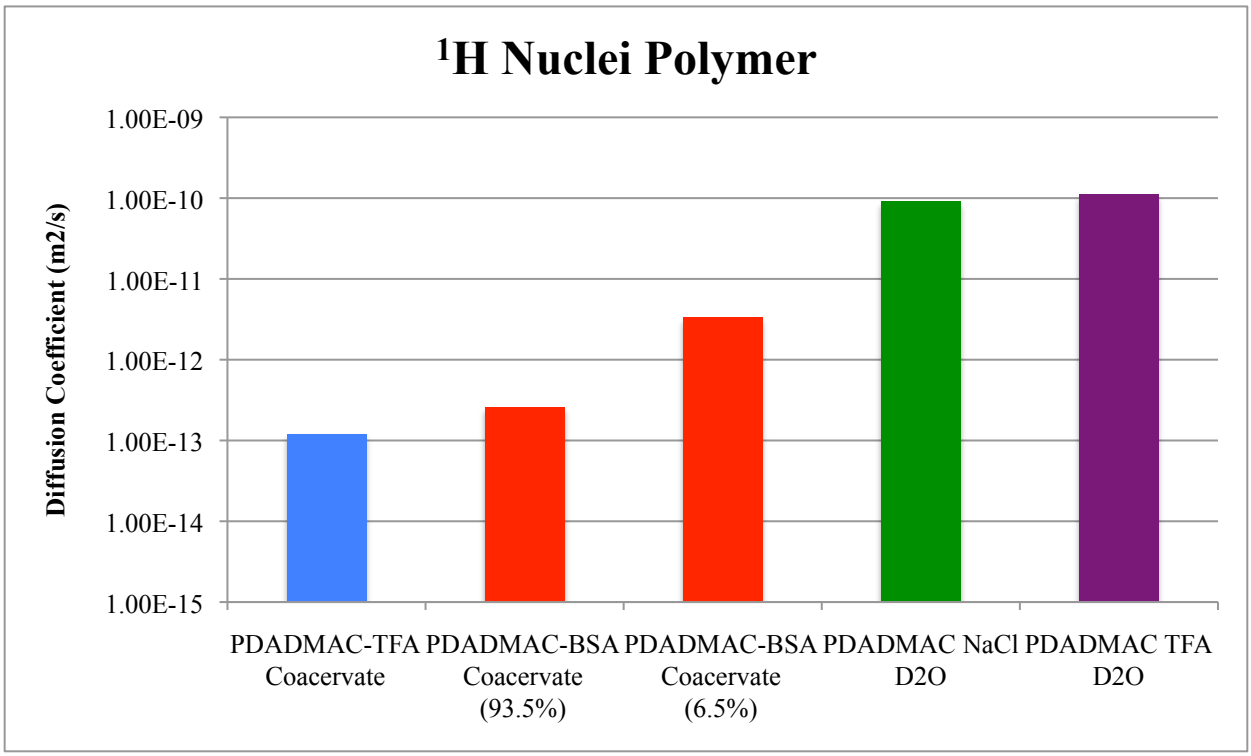

Figure 4: Comparison of diffusion coefficients for ^{1}H nuclei of polymer. Blue (left): PDADMAC-TFA-BSA coacervate, Red (second from left): less dense domain of PDADMAC-BSA coacervate, Red (third from left): breaking up of dense domains of PDADMAC-BSA coacervate, Green (second from right): PDADMAC in 0.1M NaCl, Purple (right): PDADMAC-TFA in 0.1 M in sodium trifluoroacetate.

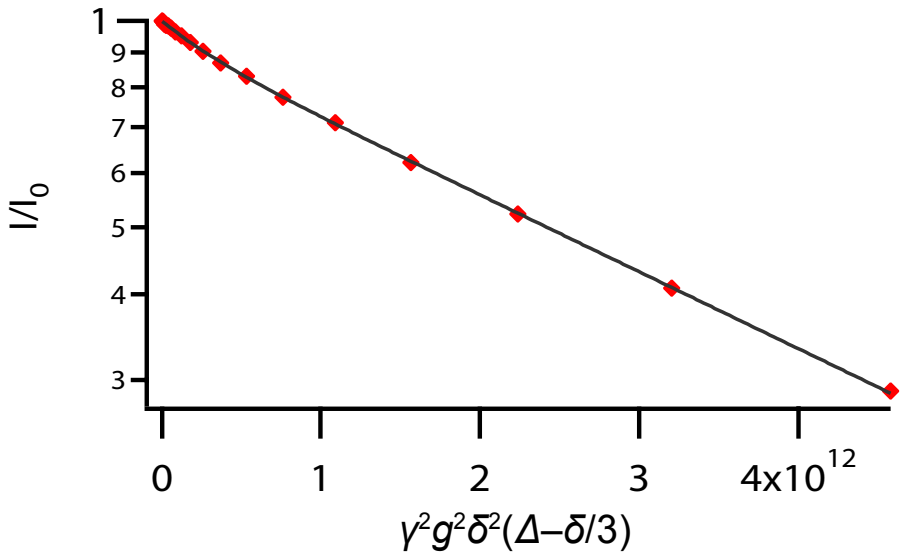

Figure 5: ^{1}H PDADMAC-BSA attenuation curve fit for two components.

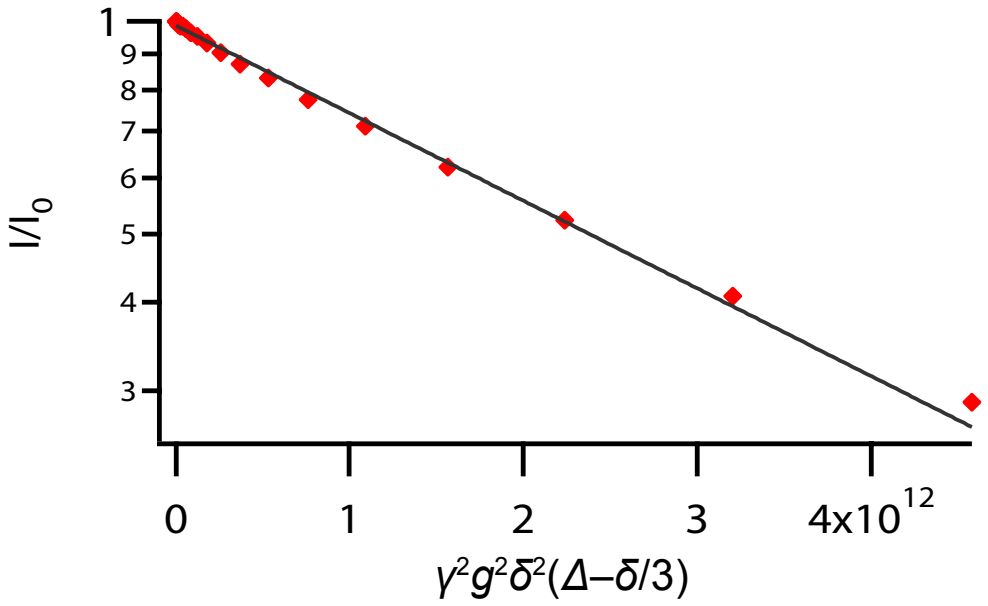

Figure 6: ^{1}H PDADMAC-BSA attenuation curve fit for one component.

^{1}HDO diffusion coefficients were compared across all samples from the integration of the frequency-domain spectrum at 4.8ppm. Diffusion coefficients were determined to have been measured primarily in the supernatant region of the tube due to the similarity of diffusion coefficients in samples of PDADMAC, BSA, and NaCl solutions (Fig. 7) Measurements from the PDADMAC-TFA coacervate showed two measured components, one in the supernatant and one in the coacervate region. The PDADMAC-BSA coacervate only showed one measured component, however it is likely that there is also a component not being measured inside the coacervate as well.

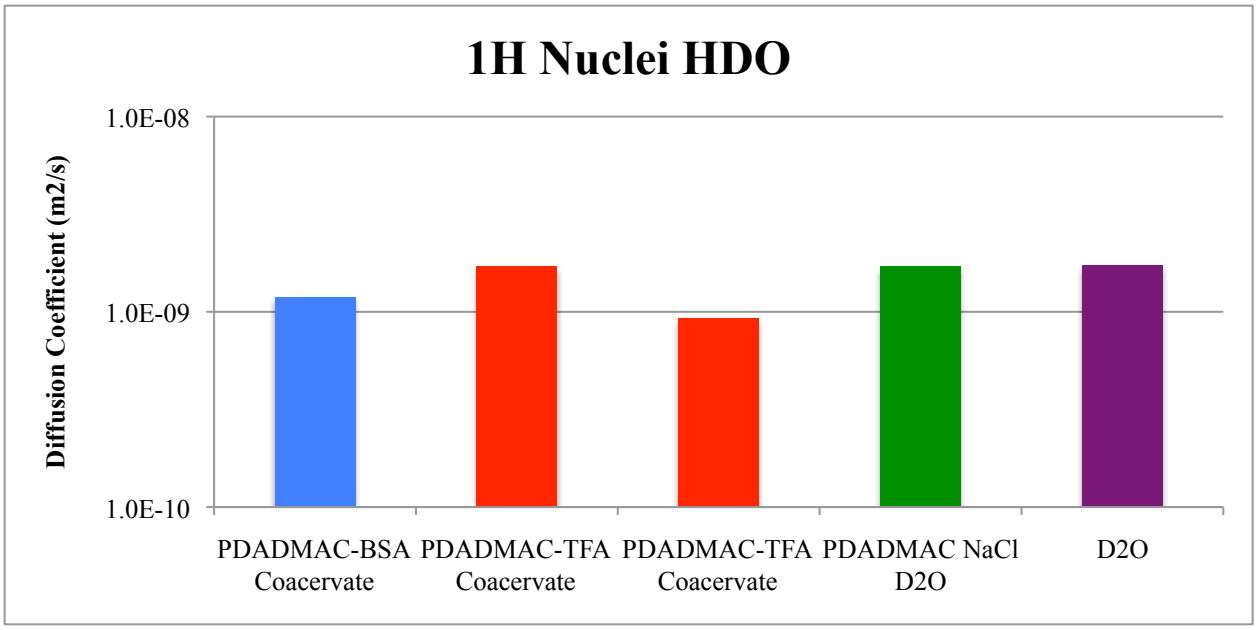

Figure 7: Comparison of diffusion coefficients for ^{1}H nuclei of water. Blue (left): PDADMAC-BSA coacervate, Red (second from left): supernatant of PDADMAC-TFA-BSA coacervate, Red (third from left): less dense domain of PDADMC-TFA-BSA coacervate, Green (second from right): PDADMAC in 0.1 NaCl, Purple (right): D_2O.

Ion diffusion measurements were primarily measured in the supernatant region of the NMR tube. ^{23}Na nuclei diffusion coefficients were relatively the same, 1.0e-9 m^2/s (Fig. 8) and information regarding ^{23}Na inside the coacervate is still unknown.. PGSTE sequences hinted that a component within the coacervate is present, but not able to be measured due to short transverse relaxation times (Fig. 9). The spectrum shows a broad component with slower motional dynamics that cannot be seen in diffusion measurements. ^{23}Na diffusion coefficients are difficult to measure due to the fast relaxation of nuclear spin states.

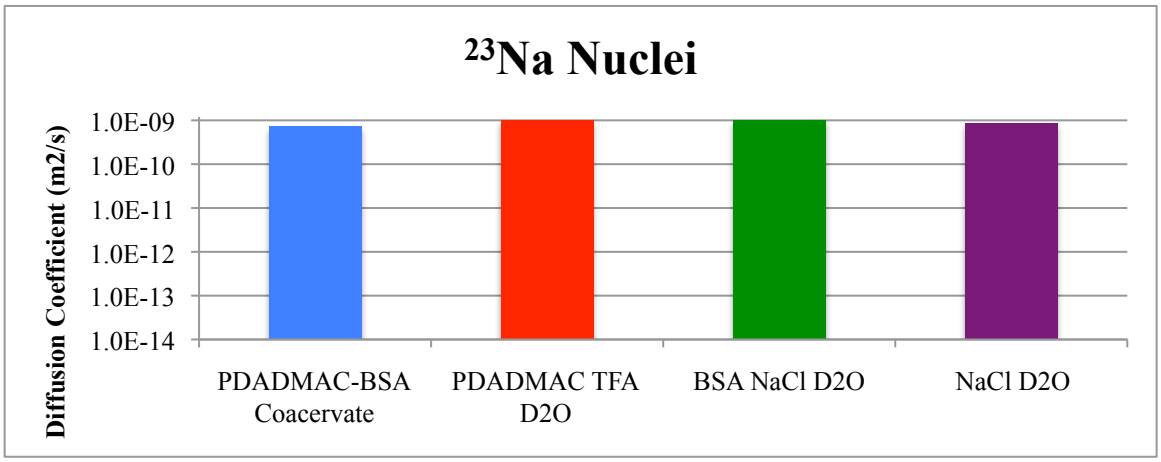

Figure 8: Comparison of diffusion coefficients for ^{23}Na nuclei

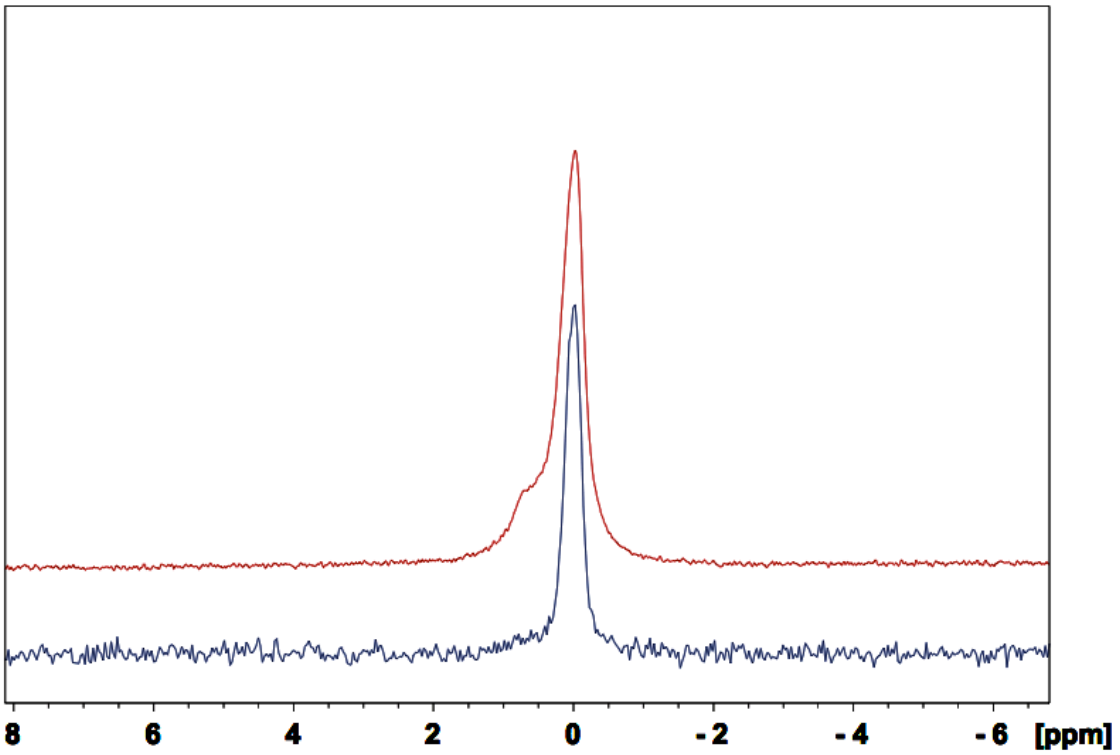

Figure 9: One-dimensional ^{23}Na NMR spectrum. Red (top): Free-induction decay hinting at a broad component and narrow component. Blue (bottom): PGSTE showing broad component is not measurable.

^{19}F diffusion measurements showed similar diffusion coefficients between PDADMAC-TFA-BSA coacervate, PDADMAC in 0.1M sodium trifluoroacetate, and 0.1M sodium trifluoroacetate hinting that ^{19}F nuclei in coacervate was primarily measured in the supernatant region. 2.7% of the PDADMAC-TFA-BSA coacervate confirmed smaller diffusion coefficients on an order of magnitude of ten than the supernatant region (Fig. 10). Due to the sensitivity of the ^{19}F chemical shift, we can see two peaks for the anion, likely due to the anions inside and outside the coacervate (Fig. 11). Diffusion coefficients were very similar to ^{23}Na nuclei and information regarding the properties of differing counterions is still unknown. However, data suggests that there is no specific binding of these ions to the macromolecule, and therefore they diffuse relatively freely based on their size.

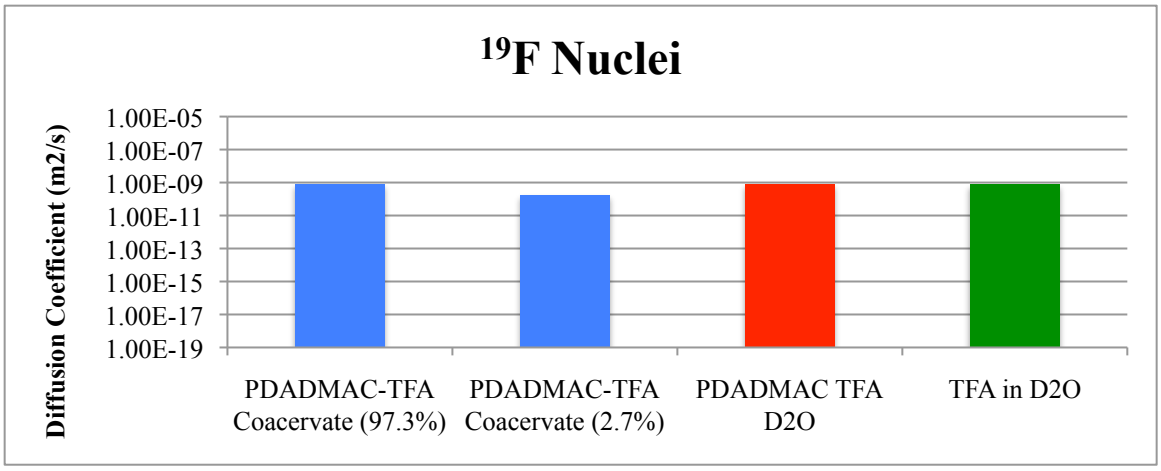

Figure 10: Comparison of diffusion coefficients for ^{19}F nuclei

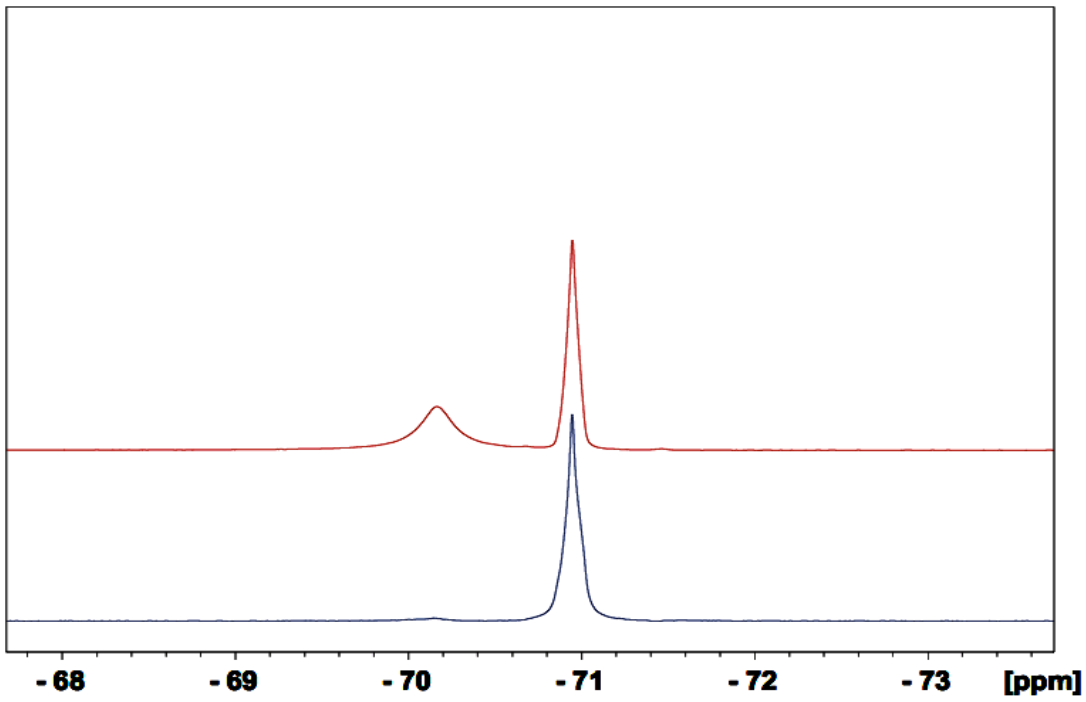

Figure 11: One-dimensional ^{19}F NMR spectrum. Red (top): Free-induction decay showing two distinct peaks, Blue (bottom): PGSTE showing too fast of relaxation of the nuclear spin state of one of the components.

^{35}Cl diffusion measurements were also conducted on the coacervate samples. These experiments are still underway, as the necessary equipment has only recently been acquired and ^{35}Cl diffusion has never been previously published in the literature.

^{35}Cl diffusion coefficients were smaller in the PDADMAC sample than in the PDADMAC-BSA coacervate. The diffusion of chloride is expected to be slower in free polymer than in coacervate due to the stronger dynamic attraction to positively charged

free polymer than to polymer inside the coacervate. However, more data regarding ^{35}Cl diffusion must be taken to confirm diffusion measurements.

Conclusion

Diffusion measurements with PFG NMR can give insight to the microstructure of polymer-protein coacervates. ^{1}H studies show similar results to those previously published, that there is heterogeneity of polymer diffusion inside the coacervate phase. ^{23}Na and ^{19}F diffusion was unable to provide any information on the coacervate phase due to the short relaxation times of the nuclei in the restricted coacervate environment. ^{35}Cl diffusion measurements are ongoing, and the preliminary data provides interesting information about ion binding to the highly-charge polymer. Diffusion measurements for ^{19}F, ^{23}Na, and ^{35}Cl have similar diffusion coefficients hinting that the ions travel at a similar rate. These measurements can help give insight into the microstructure and transport dynamics of polymer-protein coacervates, which may assist in the design of new drug delivery systems.

Acknowledgements

The Saint Mary's School of Science Summer Research Program was able to make this research possible with financial support from the Robert W. and Beverly J. Summers Scholarship. I thank Dr. Mark Lingwood for access to his start up funds and being a mentor throughout the summer. I would also like to thank the group of Louis Madsen at Virginia Tech for access to NMR instrumentation and to the Saint Mary's Undergraduate Student Research and Professional Development fund and the Faculty Development Fund for supporting travel to Virginia Tech.

References

(1) M. Malmsten. Soft drug delivery systems *Soft Matter* 2, 2006, 760–769.

(2) Wang, X., Sun, X., Jiang, G., Wang, R., Hu, R., Xi, X., Zhou, Y., Wang, S. and Wang, T. Synthesis of biomimetic hyperbranched zwitterionic polymers as targeting drug delivery carriers. J. Appl. Polym. Sci., 2013, 128: 3289–3294.

(3) Burgess, D. J.; Ponsart, S. *J.* Microencapsulation 1998, *15*, 569.

(4) Yu, X.; Li, Y.; Wu, D. *J.* Chem. Technol. Biotechnol. 2004, *79*, 475.

(5) A. Basak Kayitmazer, Himadri B. Bohidar, Kevin W. Mattison, Arijit Bose, Jayashri Sarkar, Akihito Hashidzume, Paul S. Russo, Werner Jaeger and Paul L. Dubin. Mesophase separation and probe dynamics in protein–polyelectrolyte coacervates. The Royal Society of Chemistry. Soft Matter, 2007, 3, 1064–1076.

(6) Menjoge, Amrish R., A. Basak Kayitmazer, Paul L. Dubin, Werner Jaeger, and Sergey Vasenkov. "Heterogeneity of Polyelectrolyte Diffusion in Polyelectrolyte−Protein Coacervates: AH Pulsed Field Gradient NMR Study." *The Journal of Physical Chemistry B* 112.16 (2008): 4961-966. Print.

(7) Dautzenberg, H., Görnitz, E. and Jaeger, W. (1998), Synthesis and characterization of poly(diallyldimethylammonium chloride) in a broad range of molecular weight. Macromol. Chem. Phys., 199: 1561–1571.